

SUPPORTING INFORMATION

Class I hydrophobin Vmh2 adopts atypical mechanisms to self-assemble into functional amyloid fibrils

Alfredo Maria Gravagnuolo¹, Sara Longobardi¹, Alessandra Luchini¹, Marie-Sousai Appavou⁴, Luca De Stefano², Eugenio Notomista³, Luigi Paduano¹, Paola Giardina^{1}*

¹Department of Chemical Sciences, University of Naples ‘Federico II’, Via Cintia 4, 80126 Naples, Italy

²Unit of Naples, Institute for Microelectronics and Microsystems, National Council of Research, Via Pietro Castellino 111, 80131 Naples, Italy

³Department of Biology, University of Naples ‘Federico II’, Via Cintia 4, 80126 Naples, Italy

⁴Jülich Centre for Neutron Science JCNS, Forschungszentrum Jülich GmbH, Outstation at MLZ, Lichtenbergstraße 1, 85747 Garching, Germany

Corresponding Author

*Paola Giardina. Department of Chemical Sciences, University of Naples ‘Federico II’, Via Cintia 4, 80126 Naples, Italy - Email: giardina@unina.it - Tel: +39 081 674319 - Fax +39 081 674 310

Optimization of TFA treatment

The efficiency of Vmh2 de-polymerization by TFA treatment was tested. The same amount of Vmh2 dry-aggregates (50 μg) was treated in a bath sonicator with different amounts of TFA (50 and 500 μL). After TFA removal in a stream of nitrogen, 1 mL of Na phosphate at pH 7 was added to each sample and ThT fluorescence measurements were carried out. The results indicated that an efficient de-polymerization was obtained using the highest volume of TFA (Fig. SI-2). The same experiment was carried out using a higher amount of Vmh2 (200 μg) and TFA/protein ratios spanning the same range. In this case a remarkable effect of the TFA/protein ratio was observed, however high fluorescence emission was detected even when 2 mL of TFA were used. When higher TFA/protein ratios were used inconclusive results were obtained (i.e. low final protein concentration). Therefore all the experiments were performed using the optimized TFA/protein ratio, 1 mL of TFA/100 μg of protein.

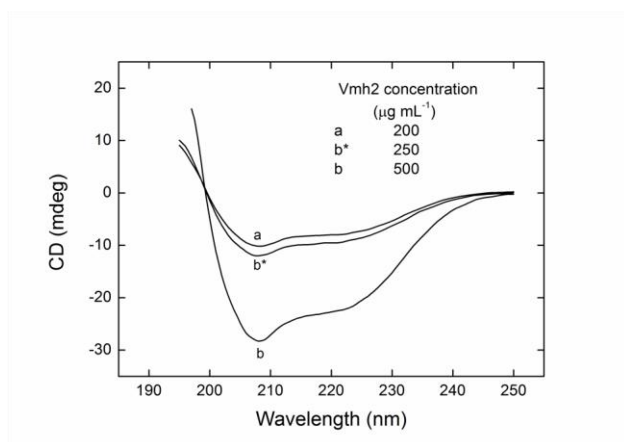


Fig. SI-1. CD spectra of Vmh2 samples prepared at 0.2 mg mL^{-1} (a) and 0.5 mg mL^{-1} (b) in 50 mM Na phosphate buffer, pH 7. The latter has been diluted twofold (b*) for an easy comparison to the sample dissolved at lower concentration.

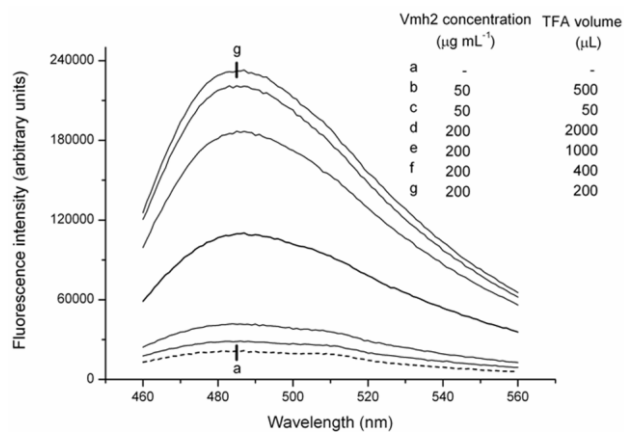


Fig. SI-2. Fluorescence spectra of ThT $30 \mu\text{M}$ in the presence of Vmh2 dissolved in 50mM Na phosphate buffer, pH 7 at different protein concentration (50 or 200 μg of Vmh2 in 1 mL buffer) previously treated with different TFA volumes.

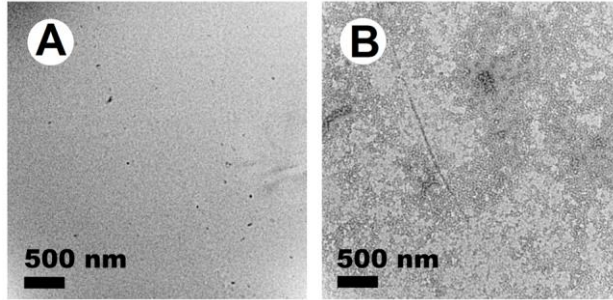


Fig. SI-3. TEM images of $50 \mu\text{g mL}^{-1}$ Vmh2 dissolved in 50 mM Na phosphate buffer, pH 7. A, sample diluted 1:50 before image acquisition, B, undiluted sample.

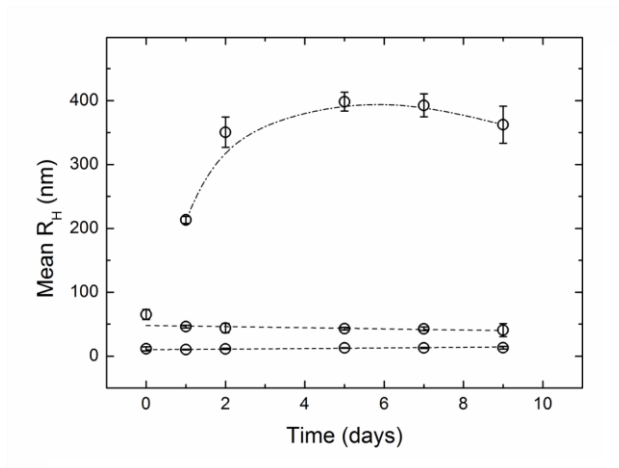


Fig. SI-4. Temporal evolution of Vmh2 ($200 \mu\text{g mL}^{-1}$) in 50mM Na phosphate buffer, pH 7, at 30 °C analyzed by DLS (lines depicted as guides for eyes), showing a third distribution of larger particles detectable after one day. Error bars representing the double of the standard deviation calculated on three measurements of the same sample.

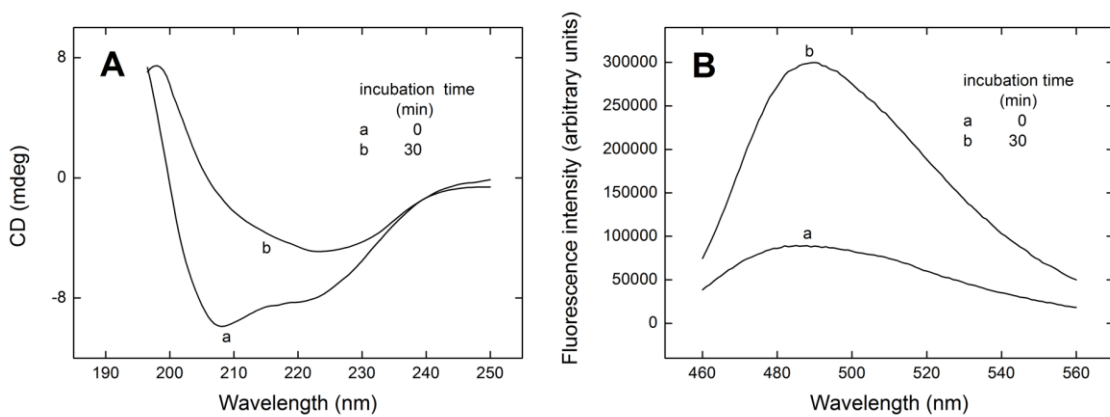


Fig. SI-5. A, CD and B, ThT fluorescence spectra of Vmh2 dissolved in 50mM Na phosphate buffer pH 7, incubated at 60 °C

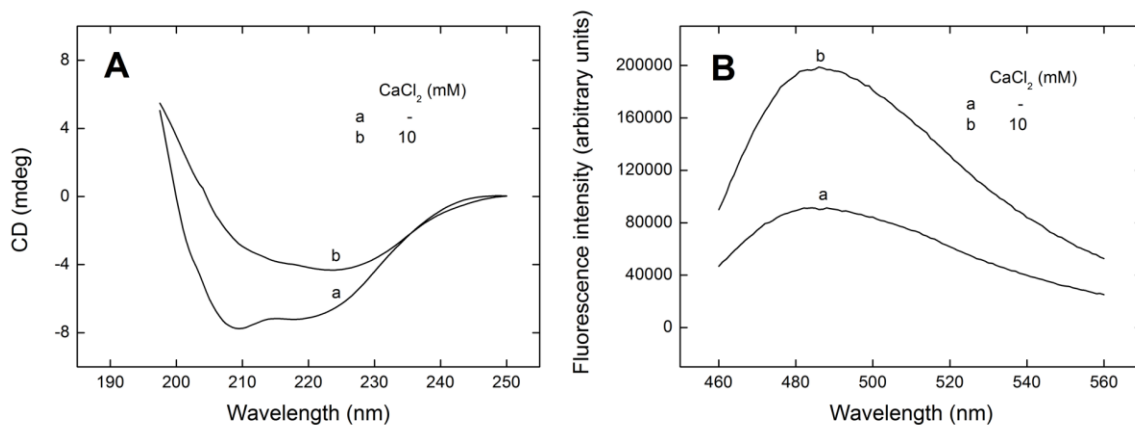


Fig. SI-6. A, CD and B, ThT fluorescence spectra of Vmh2 dissolved in 50 mM Tris HCl buffer, pH 7.0, in the presence of CaCl₂.

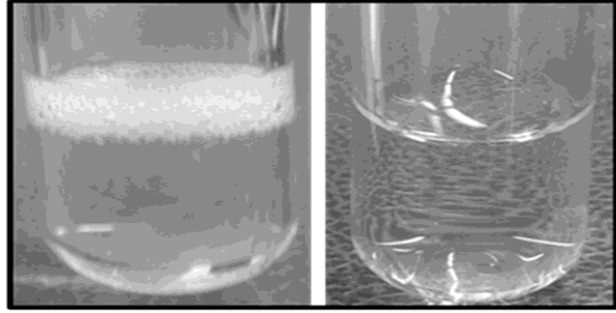


Fig. SI-7. Agitated samples, by 15 min vortexing, of Vmh2 in Na Phosphate buffer at pH 7 after 3 days (left) and 60% ethanol after 1 minute (right).

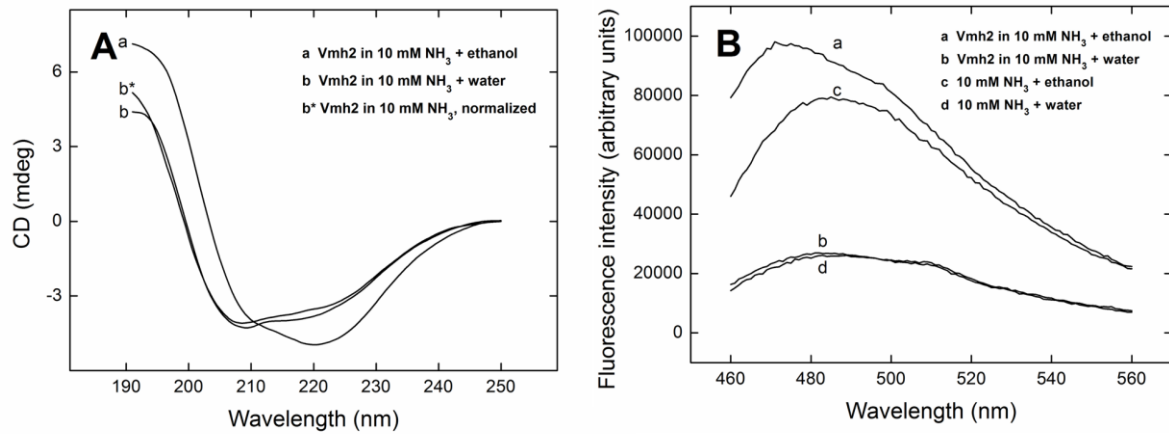


Fig. SI-8. A, CD and B, ThT fluorescence spectra of $100\mu\text{g mL}^{-1}$ Vmh2 dissolved in 10 mM NH₃ (final pH 7÷8) upon dilution, using pure ethanol up to 60% v/v, or the same volume of water.

Modeling of the Vmh2 3D structure

Fig. SI-9 shows the regions of Vmh2 that were modelled by homology and the regions that were built by the loop modeling procedure of Swiss Model server. It is worth noting that the regions modelled as loops by the server do not correspond to the hydrophobin regions defined loops L1, L2 and L3. The longest regions built by the server are the central parts of L2 and L3, whereas, in loop L1 only two short sequences upstream and downstream the second helix of the loop were modelled through the loop modeling procedure. Moreover, the residues hypothesized to be involved in interaction stabilizing loop L1 (i.e. the couples K19/D22 and D40/S81) are not included in these two regions and are also far from the regions of L2 and L3 modelled as loops.

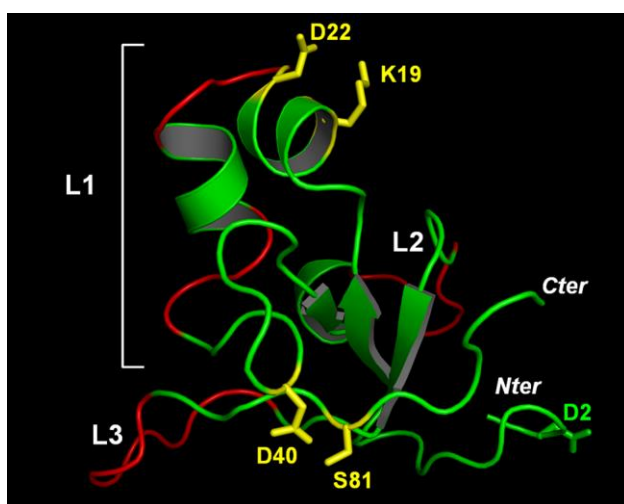


Fig. SI-9. Localization inside the model of Vmh2 of the regions modelled by homology (green) and of the regions built through the loop modeling procedure of Swiss Model server (red). Residues potentially involved in the stabilization of the compact conformation of loop L1 are shown in yellow.

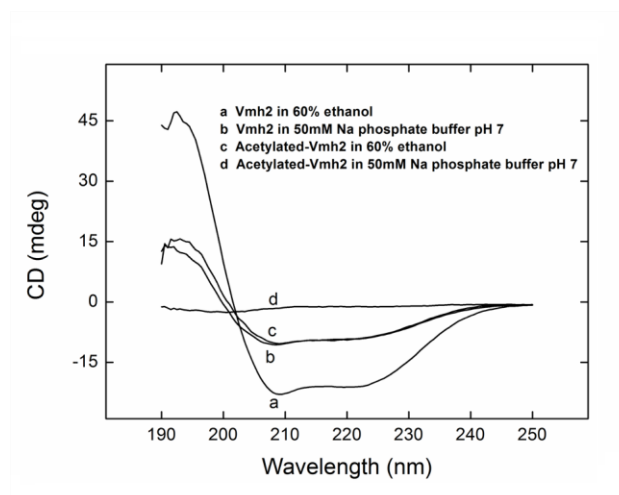


Fig. SI-10. CD spectra of $200 \mu\text{g mL}^{-1}$ Vmh2 in aqueous buffer or 60% ethanol solution, before and after acetylation of the amino groups.